30

ORIGIN OF GLOBAL MELTWATER PULSES

RICHARD G FAIRBANKS, CHRISTOPHER D CHARLES and JAMES D WRIGHT

INTRODUCTION

The fact that frequencies measured in climate records are the same as those predicted by the astronomical theory of climate change is undisputed (Hays, Imbrie & Shackleton 1976). However, the mechanisms by which these small changes in seasonal insolation are amplified into glacial cycles remain a fundamental mystery of the Earth's climate system. The Barbados postglacial sea-level record is sufficiently detailed to resolve, for the first time, the rates as well as the magnitude of continental ice melting (Fairbanks 1989, 1990) (Fig 30.1A). The Barbados meltwater discharge curve is not smooth but pulsed, with peaks at 12,000 ^{14}C years[1] and 9500 ^{14}C years (Fig 30.1B). Sea level rose more than 24 m during each of these pulses, with annual rates of sea-level rise exceeding 3 cm/yr. These enormous pulses must mark the ice-sheet response to a change in one or more of the climate amplifiers (eg, greenhouse gases and oceanic heat transports). The suspected amplifiers have different time constants and different regional sensitivities. Therefore, the discovery of both the pulsed deglaciation itself and the geographic origin of the pulses may help pinpoint the factors responsible for the timing of the large sea-level change associated with the last deglaciation, as well as the cause of previous "terminations" which recur every 100,000 ^{14}C years during the late Pleistocene Epoch (Broecker 1984).

Probably four ice sheets contribute to the shape of the global discharge curve: Laurentide; Fennoscandian; Barents; and Antarctic. Accelerator mass spectrometry (AMS) ^{14}C dating of meltwater plumes, as measured by δ^{18}O analyses of planktonic foraminifera, clearly documents the timing of the disintegration of the different continental ice sheets. Although δ^{18}O records of large meltwater plumes were discovered more than 15 years ago in continental margin sediments

[1]All ^{14}C ages are with respect to the 5568-year half-life and are uncorrected for secular changes in atmospheric ^{14}C. They are corrected for the estimated oceanic "reservoir age" of 400 years except where noted for the Southern Ocean.

Reprinted from the book *Radiocarbon After Four Decades*
edited by R. E. Taylor et al.

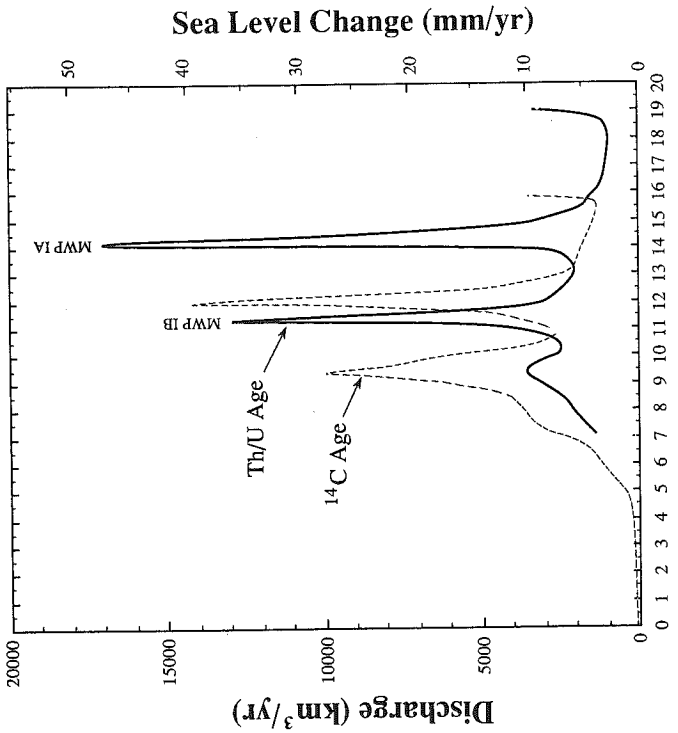

Fig 30.1B. The rate of glacial meltwater discharge calculated from the Barbados sea-level curves (from Fairbanks 1990). - - - - = the discharge curve based on the differentiation of the ^{14}C-dated sea-level curve uncorrected for secular changes in the production of ^{14}C. ——— = the discharge curve based on the differentiation of the $^{230}Th/^{234}U$-dated sea-level curve. The discharge units are cubic kilometers per year (left axis) and sea-level change in millimeters per year (right axis).

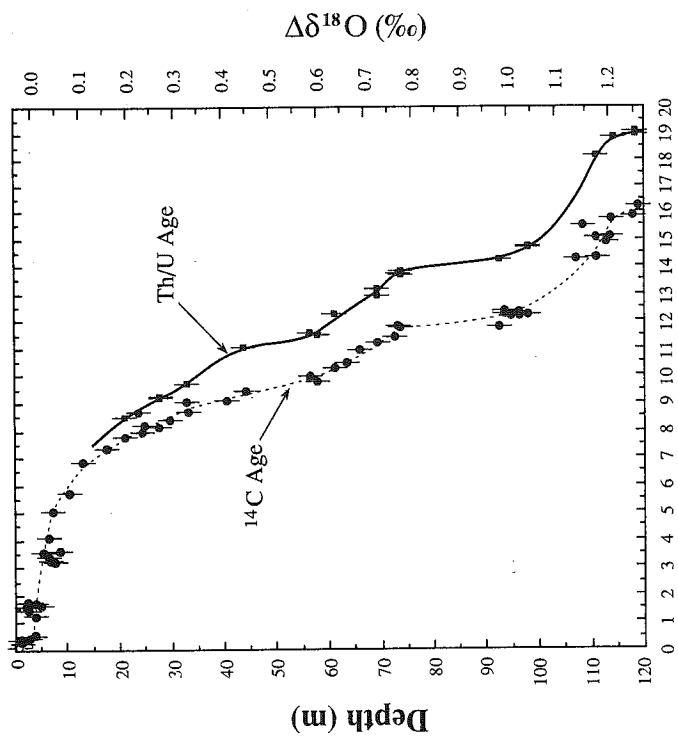

Fig 30.1A. Barbados sea-level curves based on ^{14}C-dated and $^{230}Th/^{234}U$-dated *A palmata* plotted with *A palmata* ^{14}C dates from four other Caribbean locations reported in Lighty *et al* (1982) (from Fairbanks 1990). The $^{230}Th/^{234}U$ sea-level curve is based on age determinations by mass spectrometry (squares) (Bard *et al* 1990a). Reprinted by permission of *Nature*. © 1990 MacMillan Magazines Ltd.

(Kennett & Shackleton 1975; Emiliani, Rooth & Stipp 1978; Leventer *et al* 1982), they were notoriously difficult to date because of terrestrial contamination. AMS ^{14}C dating of monospecific planktonic foraminifera from these high accumulation rate cores reveals meltwater discharge records in unprecedented detail (Broecker *et al* 1990b; Jones & Keigwin 1988). When compared with terrestrial evidence for glaciation, it is possible, for the first time, to document the sequential melting of the great continental ice sheets.

In this chapter, we examine the geographic origin of the two meltwater pulses by first documenting the timing of the meltwater plumes for the different continental ice sheets to determine which ice sheets were primarily responsible for the pulses. Analyses of the $\delta^{18}O$ of modern surface waters combined with ocean model experiments show that $\delta^{18}O$ oscillations that have the appearance of meltwater plumes can be created by ocean/climate processes. For example, changes in the production rates of North Atlantic Deep Water (NADW) may create $\delta^{18}O$ oscillations that are indistinguishable from meltwater plumes. Next, we examine the timing of several proposed amplifiers of climate change and, with the aid of General Circulation Models (GCMs), assess the regional sensitivity to these potential amplifiers. One difficulty in this approach is that comparing amplifiers of climate change to proxy records of climate change requires a standardized chronology. Most of the proxy climate records are reported in uncorrected radiocarbon years, whereas records of potential forcing, such as the CO_2 records from ice cores or astronomical calculations of local insolation, are measured or calculated in sidereal years. Here, it is important to note that the Barbados sea level record is measured in both ^{14}C years and $^{230}Th/^{234}U$ years (Bard *et al* 1990a, b; Fairbanks 1990). This new radiocarbon calibration is critical for postglacial climate research for several reasons. First, radiocarbon is not calibrated to the tree-ring chronology for the deglaciation. Second, abundant evidence from fossil trees and lake sediments indicates time intervals in the postglacial, spanning 300 to 400 years long, which had nearly constant radiocarbon ages. Third, climate researchers traditionally have assumed that sidereal and radiocarbon years are more or less interchangeable when comparing climate records (Prell 1984). The Barbados ^{14}C calibration (through $^{230}Th/^{234}U$) indicates that this assumption may be in error by as much as 2500 years (Bard *et al* 1990a, b).

COMPARISON OF GLOBAL MELTWATER DISCHARGE CURVE AND MELTWATER PULSES MEASURED IN THE CIRCUM-ATLANTIC

The meltwater discharge estimates derived from the Barbados sea-level curve must reflect the global discharge from the large continental ice sheets and has been adequately described elsewhere (Fairbanks 1989, 1990). An independent

sea-level record from New Guinea, spanning the interval 7000 to 11,000 ^{14}C years, is concordant with the Barbados results (Chappell & Polach 1991). The discharge curve has been computed in radiocarbon and $^{230}Th/^{234}U$ years (Fig 30.1B), which we equate to sidereal years based on cross-calibration to the dendrocalibrated radiocarbon time scale (Stuiver *et al* 1986) and annual band counting in living corals (Bard *et al* 1990a, b; Edwards, Taylor & Wasserburg 1988). The two prominent peaks in meltwater discharge, termed meltwater pulse (MWP) IA and IB, are dated at 12,000 ^{14}C years (14,100 $^{230}Th/^{234}U$ yrs) and 9500 ^{14}C years (11,300 $^{230}Th/^{234}U$ yrs), respectively. The MWPs reached values of 17,000 km^3/yr for MWP-IA and 13,000 km^3/yr for MWP-IB.

Since the Barbados sea-level and discharge curves were derived, numerous meltwater plumes have been measured in the circum-North Atlantic and Gulf of Mexico and dated by AMS ^{14}C. The plumes are identified by anomalously low $\delta^{18}O$ values measured in high-accumulation-rate cores along the continental margins of the North Atlantic. Figure 30.2 illustrates the $\delta^{18}O$ records for six cores in the circum-Atlantic which are reported to be examples of meltwater plumes from the Barents, Fennoscandian and Laurentide ice sheets. There is a clear distinction between the timing of meltwater plumes from these three ice sheets. The results from two cores in the Norwegian Sea (V27-60 and PS21295-4) document a meltwater plume centered between 15,500 and 14,500 ^{14}C years (Jones & Keigwin 1988; Lehman *et al* 1991). This meltwater plume is believed to mark the early disintegration of the Barents ice sheet (Jones & Keigwin 1988). A $\delta^{18}O$ record from the North Sea (Troll 3.1), adjacent to the Fennoscandian ice sheet, documents a meltwater plume between 14,200 and 13,200 ^{14}C years (Lehman *et al* 1991). The most dramatic and best-dated MWP is found in the Gulf of Mexico, recording an MWP centered at 12,000 ^{14}C years (Broecker *et al* 1990b). In several of the Gulf of Mexico records and all MWP records outside of the Norwegian Sea, a dramatic $\delta^{18}O$ decrease occurs between 10,000 and 9000 BP. The shift is generally associated with warming in the North Atlantic, so it does not usually result in an "overshoot" of $\delta^{18}O$ values. Thus, the MWP after 10,000 ^{14}C years is difficult to define by available $\delta^{18}O$ records alone.

Fig 30.2. Oxygen isotope records of planktonic foraminifera showing pulsed and sometimes sequential melting of different continental ice sheets plotted on a map of observed free-air gravity anomalies over Canada and Fennoscandia (from Peltier 1990). The AMS-^{14}C-dated meltwater plumes are from Broecker *et al* (1990b) Gerg 87G13-31; Jones and Keigwin (1988) PS21295-4; Lehman *et al* (1991) V27-60, V28-14 and Troll 3.1 (shallow-water benthic foraminifera were analyzed in this core); Bard *et al* (1987) SU81-18; Labracherie *et al* (1989) MD84-551.

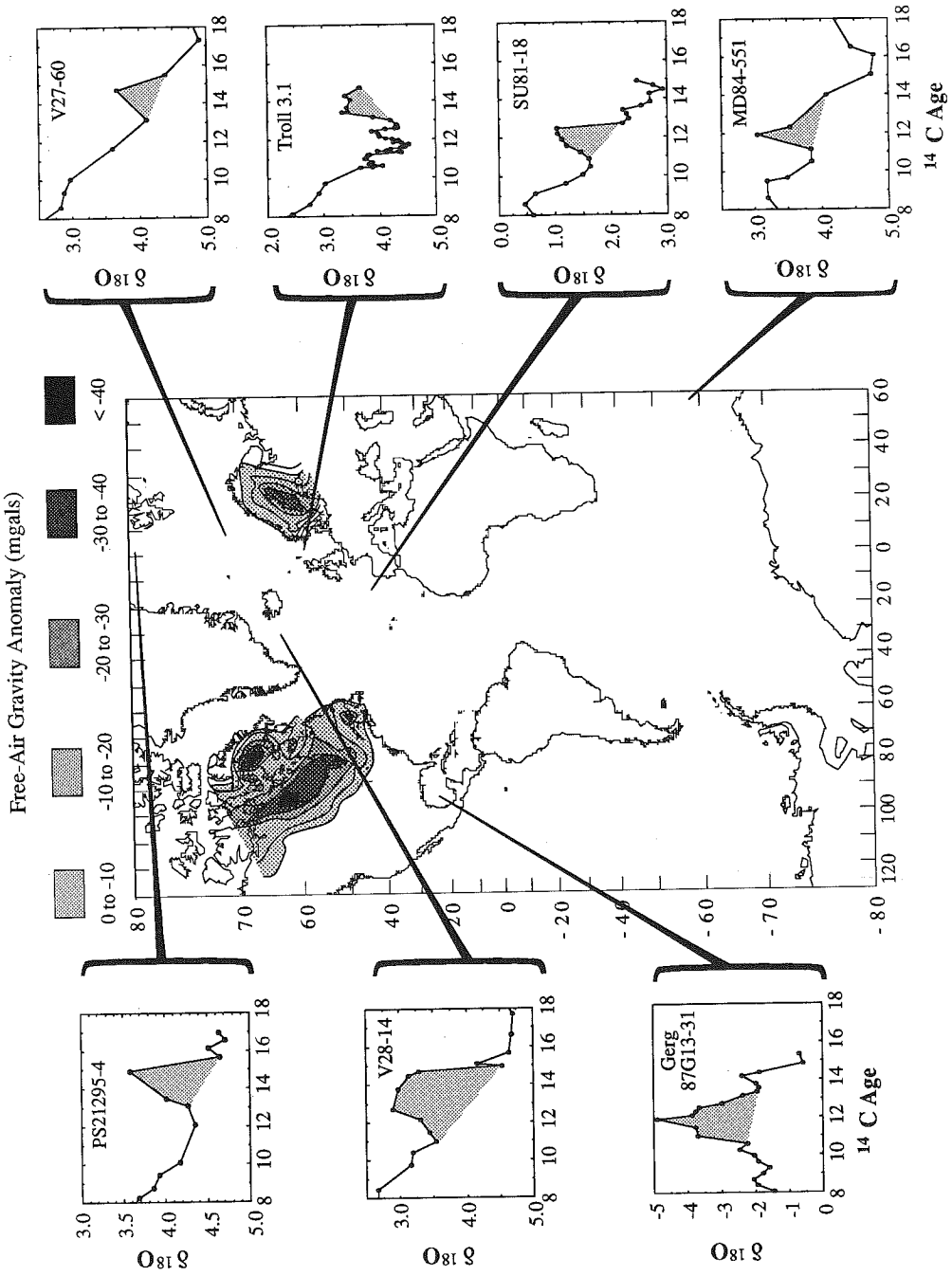
Free-Air Gravity Anomaly (mgals)
0 to -10
-10 to -20
-20 to -30
-30 to -40
< -40
V27-60
Troll 3.1
SU81-18
MD84-551
PS21295-4
V28-14
Gerg 87G13-31
δ 18O
14 C Age

It is important to note that small shifts in the isotherms and/or changes in salinity unrelated to MWPs can produce a $\delta^{18}O$ anomaly indistinguishable from glacial meltwater. Changes in the seasonal flux of a foraminiferal species can also produce a $\delta^{18}O$ transient. Examination of the predicted $\delta^{18}O$ of calcite for the modern surface ocean shows the sensitivity of this tracer to changes in the evaporation/precipitation balance and water mass mixing. It is well known that the $\delta^{18}O$ of foraminiferal calcite tests are predominantly a function of temperature and $\delta^{18}O$ of sea water, as well as some minor effects associated with the ecology and life cycles of different species. Figure 30.3A shows an example of the modern salinity field for northern hemisphere spring (March, April, May), which was used to compute the $\delta^{18}O$ of sea water for this season based on measurements of the $\delta^{18}O$-salinity relationship for all of the major salinity gradients (Fig 30.3B). A set of seven $\delta^{18}O$-salinity equations was used to compute the

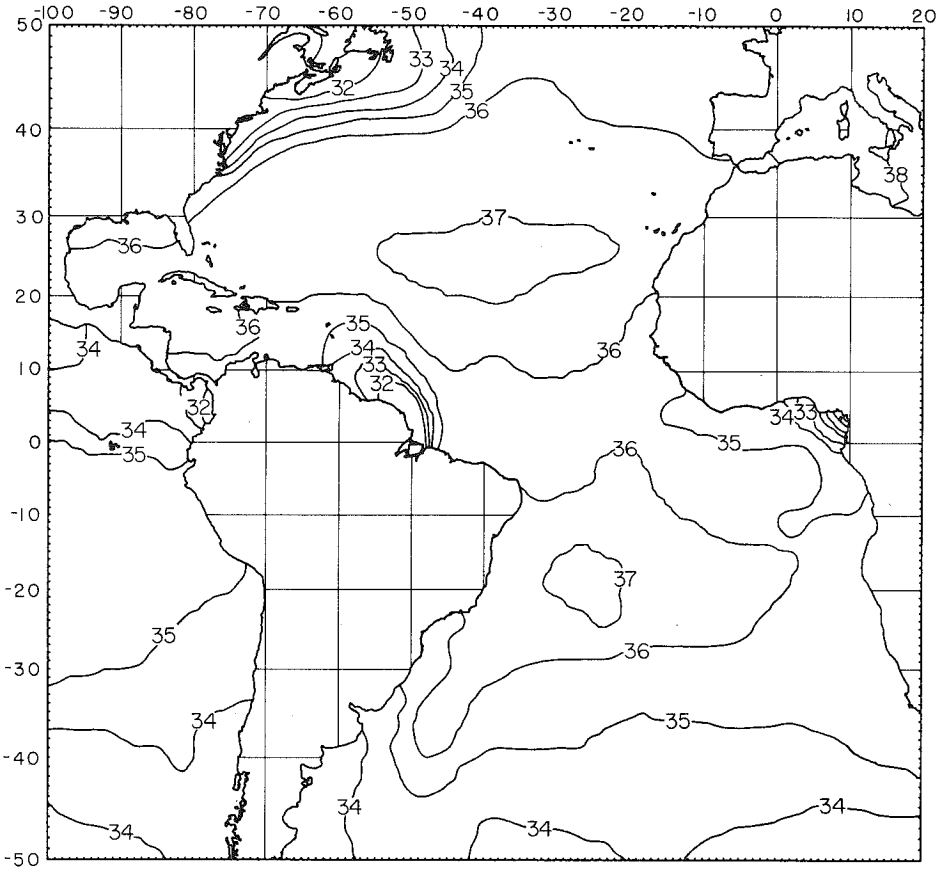

Fig 30.3A. Map of modern Atlantic surface water salinity averaged for the months of March, April and May (from Levitus 1982)

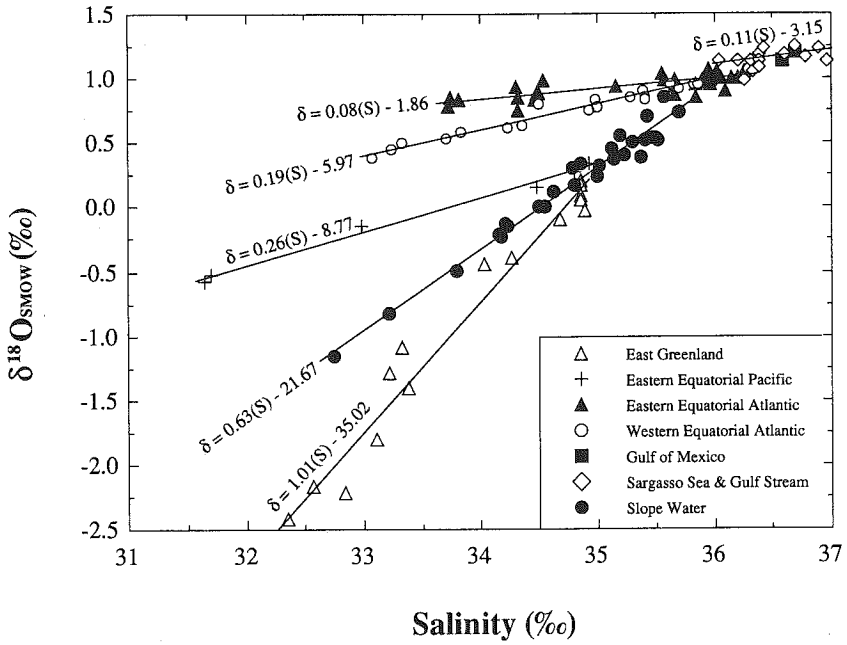

Fig 30.3B. Plots of $\delta^{18}O$ and salinity measurements across all major salinity gradients in the Atlantic and eastern tropical Pacific (Fairbanks, ms in preparation)

surface-water $\delta^{18}O$ on a 1° × 1° grid (Fairbanks, ms in preparation) for each season. Combining the estimated $\delta^{18}O$ of sea water with the measured monthly temperature from Levitus (1982) (Fig 30.3C), we computed the estimated $\delta^{18}O$ of calcite for each month. Figure 30.3D is the computed annual average $\delta^{18}O$ of calcite, and illustrates that it is easy to create $\delta^{18}O$ transients that are not MWPs. In the subpolar region, the effect of decreasing temperature on the $\delta^{18}O$ of calcite dominates the opposite effect of decreasing $\delta^{18}O$ of sea water poleward. In the polar waters, where surface water is freezing, the salinity has a greater influence on the isopleths of $\delta^{18}O_{calcite}$. This relationship adds some confidence to the meltwater origin of the Fram Strait core PS21295-4 (Fig 30.2). However, the best way to verify that a $\delta^{18}O$ anomaly is an MWP is to trace its increasing amplitude toward the source. The 4‰ $\delta^{18}O$ pulse from the Gulf of Mexico (Gerg 87G13-31) is the only MWP that is of indisputable origin. Although all of the other $\delta^{18}O$ anomalies in Figure 30.2 have been reported in the literature as MWPs, their relationship to meltwater awaits verification.

CLIMATE FORCING FACTORS

According to the astronomical theory of climate change, the Pleistocene ice ages were caused primarily by changes in the seasonal distribution of incoming solar

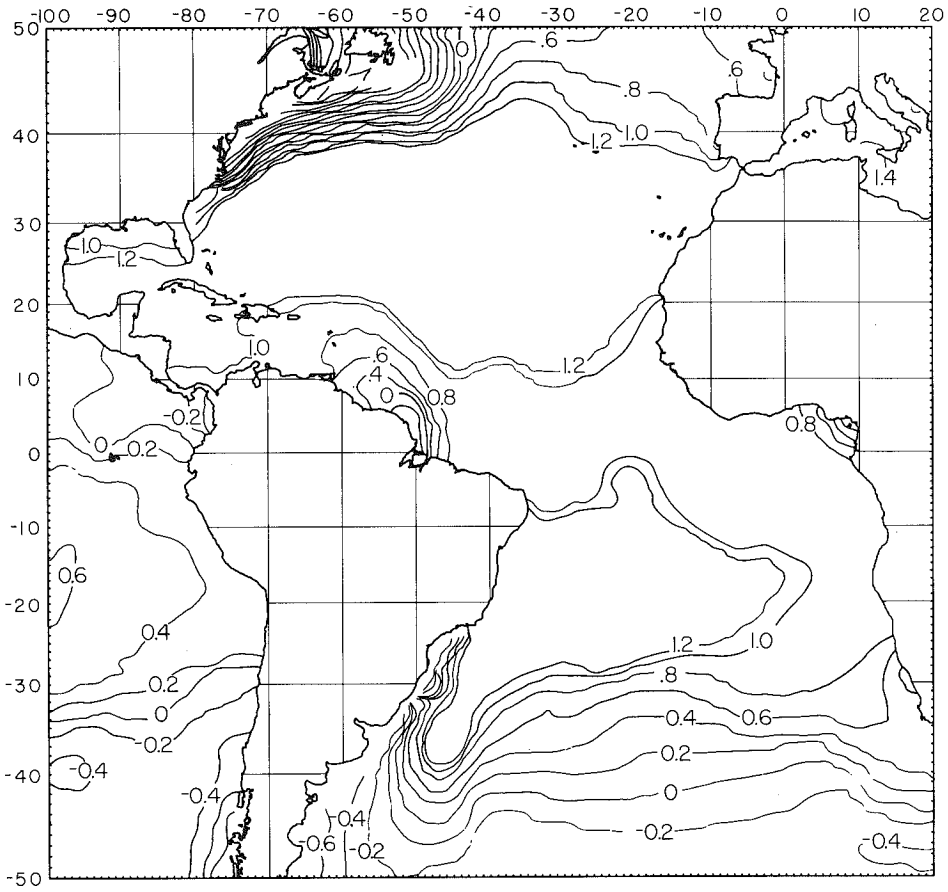

Fig 30.3C. The estimated $\delta^{18}O$ of modern Atlantic surface water averaged for the months of March, April and May. The map is based on the salinity *vs* $\delta^{18}O$ equations in Figure 30.3B applied to the salinity map in Figure 30.3A.

radiation associated with orbital variations (Milankovitch 1941). The northern hemisphere ice sheets accumulate in the 40°–80° N latitude range, whereas the Antarctic ice sheet is located poleward of 70° S. Insolation changes associated with the 41,000-year tilt cycle increase poleward in both hemispheres, while the 23,000-year precessional cycle dominates insolation changes at middle and low latitudes and is out of phase between hemispheres. Figure 30.4 shows the summer insolation at 50°, 60°, 70° and 80° N latitude, as calculated from the equations of Berger (1978). Summer insolation between 24,000 and 11,000 years increases by 11% at 50°N compared to 15% at 80°N. The relationship between insolation and a "filtered" sea-level curve is reasonably good for the last deglaciation, now that the sea-level curve is corrected to sidereal years. However, we know from comparison of insolation to the present-day sea level,

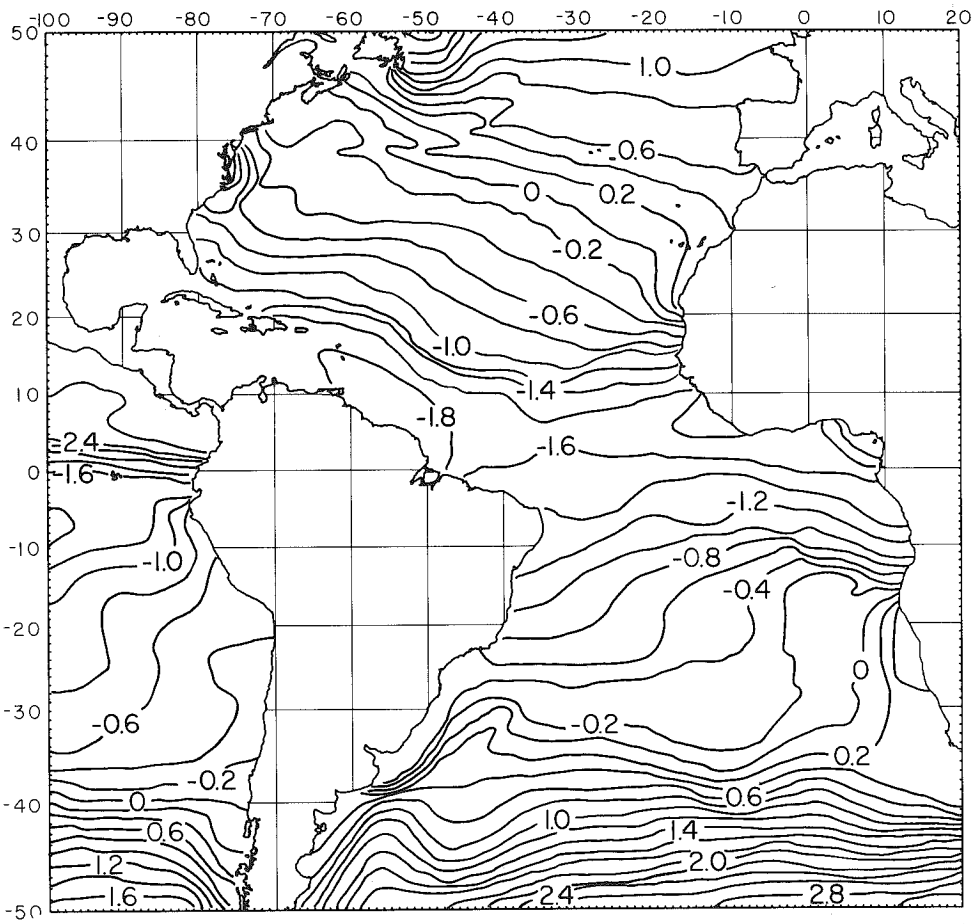

Fig 30.3D. The predicted annual average $\delta^{18}O$ of calcite is based on the "paleo-temperature" equation of Epstein *et al* (1953) using the 1° × 1° gridded temperature and $\delta^{18}O_{sea\ water}$ values.

as well as from longer records of sea level, that insolation alone does not correspond directly to ice volume or its sea-level equivalent. In the next section, we examine the timing and regions of influence of two suspected amplifiers of the insolation forcing function, in order to assess their possible roles in generating the meltwater discharge curve (Fig 30.1B).

One popular explanation for the non-linear response of climate change is variability in the production rate of NADW (Stommel 1961; Rooth 1982; Broecker, Peteet & Rind 1985; Bryan 1986; also see Broecker & Denton 1989, for a review). Several characteristics of the NADW thermohaline circulation provide the basis for this hypothesis. The process of NADW formation leads to excessive heat loss from the ocean to the atmosphere in the northern hemisphere

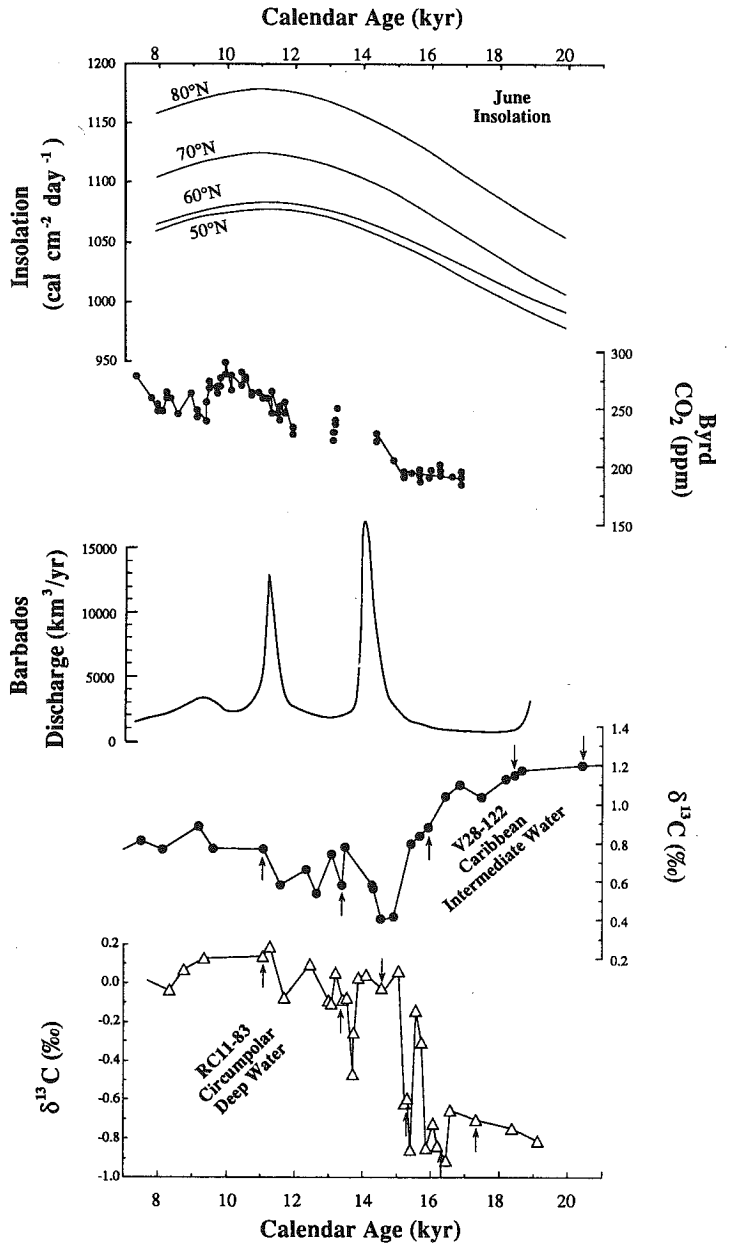

Fig 30.4. Record of atmospheric CO_2 from Byrd (Antarctica) polar ice core (Neftel *et al* 1988; Staffelbach *et al* 1991) compared to global meltwater discharge curves (Fairbanks 1990) and northern hemisphere summer insolation (Berger 1978), all reported in calendar or $^{230}Th/^{234}U$ years. Comparison of the Southern Ocean record of NADW flux (core RCl1-83 benthic foraminifera $\delta^{13}C$ record) with a mid-depth $\delta^{13}C$ time series of Atlantic intermediate water chemistry (core V28-122 benthic foraminifera $\delta^{13}C$ record) (Charles & Fairbanks, ms) adjusted to calendar years using the ^{14}C calibration of Bard *et al* (1990a, b), showing the coincidence of NADW production and deglaciation. AMS-^{14}C-dated levels are indicated by arrows.

winter. The heat released upon NADW formation is equivalent to 35% of the solar energy incident on the North Atlantic polar latitudes today, and therefore, changes in the production of NADW might explain large, rapid changes in European continental climate (Broecker & Denton 1989). NADW also provides a crucial source of heat and salt to other oceans, especially the Southern Ocean, where a convergence of oceanic heat is required to melt sea ice on an annual basis (Gordon 1986). Further, NADW variability would affect oceanic nutrient and CO_2 distributions on a global scale, and therefore, may indirectly change atmospheric CO_2 content. Finally, modeling studies suggest that it may be possible for the NADW cell to switch catastrophically between stable on and off modes (Bryan 1986; Manabe & Stouffer 1988; Maier-Reimer & Mikolajewicz 1989).

Changes in the flux of North Atlantic Deep Water as measured in the Southern Ocean

Although investigators of deep-sea sediment cores in the North Atlantic have tried to delineate the history of NADW production during the last deglaciation, the chronology of the records analyzed and the generalities of the results remain uncertain (Mix & Fairbanks 1985; Boyle & Keigwin 1987; Jansen & Veum 1990; Keigwin & Jones 1989). Oppo and Fairbanks (1987, 1990) and Charles and Fairbanks (ms) show that the Southern Ocean is one of the best regions in which to study the details of NADW variability and the consequent climatic effects. Taking advantage of the global-scale mixing of deep water that occurs in the Antarctic Circumpolar Current, Charles and Fairbanks (ms) used benthic foraminiferal $\delta^{13}C$ from a Southern Ocean core (RC11-83, 41°36′S; 09°48′E, 4718 m) with a high sedimentation rate to document the timing of NADW flux from the Atlantic Ocean during the last deglaciation (Fig 30.5). The deglacial time scale for RC11-83 is derived from 11 AMS ^{14}C dates on seven levels in the core (Charles & Fairbanks, ms). The AMS ^{14}C measurements were made at the University of Arizona NSF Accelerator facility for Radioisotope Analysis by A J T Jull and D J Donahue.

The RC11-83 benthic $\delta^{13}C$ record (Fig 30.4) indicates that deglacial changes in the nutrient chemistry of the deep Southern Ocean were rapid and large. An abrupt 1‰ shift from low values characteristic of glacial conditions to high values occurred from 12,600 to 12,200 ^{14}C years. This rapid rise in Southern Ocean $\delta^{13}C$ values was most likely associated with a change in status of NADW, switching from the "off" mode to the "on" mode. The RC11-83 record also shows significant oscillations superimposed on this basic NADW off-on switch. A prior oscillation occurred between 13,300 ^{14}C years and 12,800 ^{14}C years, and a low $\delta^{13}C$ event occurred at 11,800 ^{14}C years.

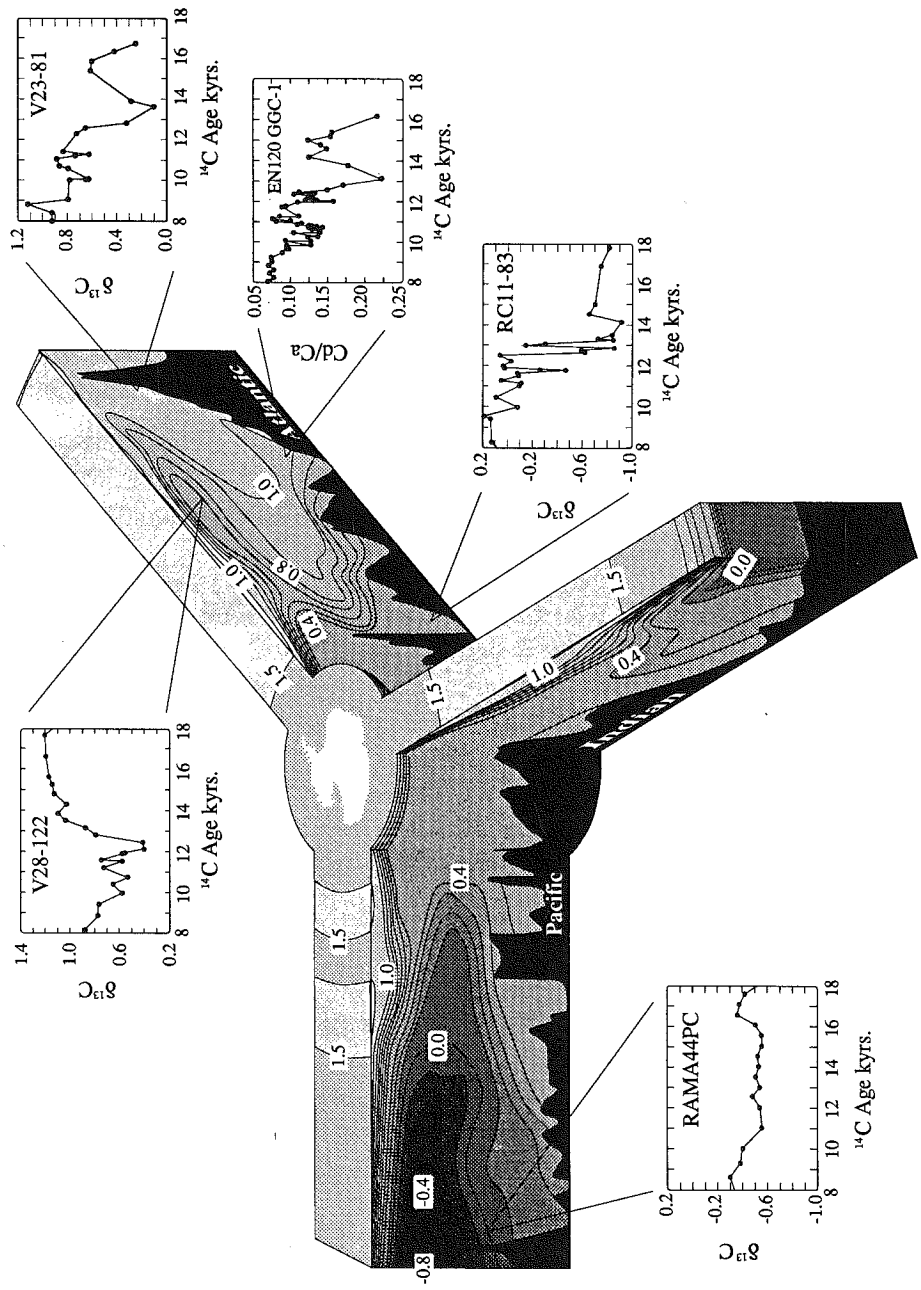

Fig 30.5. GEOSECS $\delta^{13}C$ data from the different ocean basins (Kroopnick 1985) with postglacial times series of $\delta^{13}C$ in sediments dated by AMS ^{14}C for the North Atlantic (Jansen & Veum 1990), intermediate-depth Atlantic (Oppo & Fairbanks), Southern Ocean (Charles & Fairbanks, ms) and Pacific Ocean (Keigwin 1987). Also shown for the North Atlantic are Cd/Ca in sediments dated by AMS (Boyle & Keigwin 1987).

Comparison with other detailed deglacial records from the deep North Atlantic shows significant differences for the interval from 16,000 to 13,500 ^{14}C years (Fig 30.5). The North Atlantic records show this region was first inundated with NADW between 17,000 and 15,000 ^{14}C years, followed by minimum NADW between 14,000 and 13,000 ^{14}C years, reaching or exceeding glacial $\delta^{13}C$ values (Boyle & Keigwin 1987; Jansen & Veum 1990). The striking transition from nutrient enrichment (low $\delta^{13}C$) to nutrient depletion (high $\delta^{13}C$), which is dated between 12,600 and 12,200 ^{14}C years in RC11-83, is apparent in all three records (Fig 30.5). Another step in the same direction, but with much lower amplitude, is apparent from about 10,000 to 9,000 ^{14}C years.

The $\delta^{13}C$ records that monitor mid-depth North Atlantic water provide further documentation of a rapid change in upper NADW nutrient chemistry from 14,000 to 12,400 ^{14}C years (Fig 30.5). In these records, the sense of change prior to 12,200 ^{14}C years is opposite to that of the deep Atlantic. Whereas relative nutrient depletion prevailed during glacial periods, a shift to more nutrient-rich conditions occurred at 12,700 ^{14}C years, synchronous with the timing of deep-ocean change. The inverse mid-depth and deep-Atlantic signals could both reflect the same phenomenon if, as in today's ocean, relatively nutrient-rich water from the Southern Ocean were drawn northward across the equator at mid-depth by the removal of surface and thermocline water to form southward-flowing NADW.

Where the various North Atlantic nutrient proxy records disagree, we suggest that RC11-83 should be taken as the more comprehensive measure of NADW flux variability for two reasons. First, deglacial sedimentation rates in RC11-83 are highest. Second, RC11-83 $\delta^{13}C$ values presumably monitor the flux of NADW relative to Pacific and Indian outflow, while mixing between NADW and Southern Ocean Water may vary independently of NADW flux in some North Atlantic locations. This issue is important for the interval from 17,000 to 15,000 ^{14}C years, because the North Atlantic records indicate a switch from high to low nutrients, suggesting that the initiation of NADW began 3000 years earlier than indicated by the Southern Ocean record. The RC11-83 record, on the other hand, shows more uniformly low $\delta^{13}C$ values until 13,000 ^{14}C years, indicating minimal NADW flux throughout the glacial period. This issue is also important for characterizing the Younger Dryas interval (11,000 to 10,000 ^{14}C years), the period during which, according to previous interpretations of a Bermuda Rise core (Boyle & Keigwin 1987), NADW production was temporarily reduced. The Southern Ocean record does not show an anomaly during this period, implying that the total flux of NADW may not have varied significantly. Thus, North Atlantic cores situated in the mixing zones between

water masses may be too sensitive to small circulation changes to document accurately net changes in the NADW flux.

It is possible, however, that deviations from the simple mixing models for Circum-Polar Deep Water (CPDW) $\delta^{13}C$ can occur. For example, some evidence suggests that CPDW $\delta^{13}C$ was lower than in the deep Pacific during glacial periods, and this distribution of $\delta^{13}C$ cannot be easily explained by mixing alone unless Indian Ocean deep water compensated for the relatively nutrient-depleted Pacific water mixing in the circumpolar region. One could also invoke non-conservative effects that are unique to the Antarctic, such as proposed by Boyle (1990). A more serious problem is the observation that Cd/Ca ratios in benthic foraminifera from Southern Ocean cores do not increase nearly as much as the $\delta^{13}C$ might predict during glacial periods (Boyle 1991). We have no definitive answer for why the Southern Ocean $\delta^{13}C$ at times might be lower than the Pacific, and the discrepancy between $\delta^{13}C$ and Cd/Ca demands more research into the decoupling of these tracers from the nutrient elements in the Southern Ocean (eg, see Charles & Fairbanks 1990). Nevertheless, we make the simplest interpretation that seems justified from the modern distribution of $\delta^{13}C$ (Kroopnick 1985) and the core-top calibration of benthic foraminifera $\delta^{13}C$ in deep water (Belanger, Curry & Matthews 1981): a strong relative contribution of NADW is the only means for increasing CPDW $\delta^{13}C$ above Pacific (mean ocean) values.

Ice-core record of atmospheric CO_2 change

Antarctic ice-core specialists have emphasized the primary role of atmospheric CO_2 content in amplifying the glacial-interglacial cycles (Lorius *et al* 1990). The Antarctic CO_2 results are cited as an important independent calibration for the so-called CO_2 amplifier factor, which is incorporated in GCMs. Evaluating the magnitude of the CO_2 amplifier is at the heart of climate research today. Recently, the deglacial ice from Vostok (Antarctica) and Dye 3 (Greenland) ice cores have been reanalyzed for atmospheric CO_2, and additional data have been added to the Byrd (Antarctica) record in the critical deglacial interval (Barnola *et al* 1991; Staffelbach *et al* 1991). Re-evaluation of the air dating at Vostok indicates that the age difference between air and ice is about 6000 years during the coldest periods, rather than 4000 years as previously estimated (Barnola *et al* 1991). The long and variable closure age and poor sampling resolution of Vostok make the record unsuitable for comparison to the high-resolution ocean/climate records from the Southern Ocean, North Atlantic and Barbados. However, new data from Dye 3 and Byrd (Antarctica) are critical for this comparison (Fig 30.4).

Previous results from Dye 3 indicated that the CO_2 shift from glacial to postglacial occurred in approximately 650 years (Stauffer *et al* 1985). The new CO_2 measurements in this interval show anomalously high CO_2 concentrations and high variability between samples, characteristic of problems associated with melt layers (Staffelbach *et al* 1991). In their original paper, Stauffer *et al* (1985) argued for the validity of the rapid shift in CO_2 based on the fact that the shift occurred within an interval of anomalously low $\delta^{18}O$. This interval of low $\delta^{18}O$, also recognized in the Camp Century (Greenland) ice core, is similar to the interval interpreted as the Younger Dryas (which has been interpreted as an unusually cold interval) (Dansgaard, White & Johnson 1989). Interestingly, this is the same interval which Fairbanks (1990) reinterpreted to be a warm interval correlative with MWP-IA. It is now clear from the composite CO_2 data set for Dye 3 that the highest CO_2 values, exceeding 350 ppm, and the intervals of greatest variability occur in the two core sections with lowest $\delta^{18}O$ values (Staffelbach *et al* 1991). Regardless of the stratigraphic interpretation for this specific interval, the CO_2 results from Dye 3, and even CO_2 data sampled in intervals with low $\delta^{18}O$, are now suspect.

By default, we are left with only those CO_2 results from Byrd ice core, which, unfortunately, are dated by ice-flow models. New CO_2 data from the deglacial section of Byrd confirm a slow increase (Staffelbach *et al* 1991) from 1350 to 1000 m deep. According to the age model of Paterson and Hammer (1987) the glacial to postglacial change in CO_2 corresponds to the time interval from 20,000 to 10,750 BP. Based on their new CO_2 data for Dye 3 and Byrd, Staffelbach *et al* (1991) conclude that the glacial-to-postglacial rise in CO_2 (190–270 ppm) occurred slowly over a 10,000-year interval, and not rapidly over a 650-year interval, as they previously reported (Stauffer *et al* 1985) (Fig 30.4).

DISCUSSION

Increasing CO_2 and insolation are predicted to cause greatest climate changes in the polar regions. According to GCM simulations, the northern hemisphere polar region is most affected by an increase of atmospheric CO_2 (Fig 30.6). The difference in air temperatures for a $2 \times CO_2$ simulation is estimated to be as much as 4°C for North America for today's climate (Stouffer *et al* 1989). However, the CO_2 data from Byrd show only a 15% increase immediately prior to MWP-IA, thus implying extremely small thermal consequences for the Laurentide ice sheet.

Taken at face value, the AMS-^{14}C-dated meltwater plumes in the circum-Atlantic indicate sequential melting of the northern hemisphere ice sheets starting with the Barents, followed by the Fennoscandian and, finally, the Laurentide ice sheet (Fig 30.2). This north to south deglaciation is consistent with the ICE-3 recon-

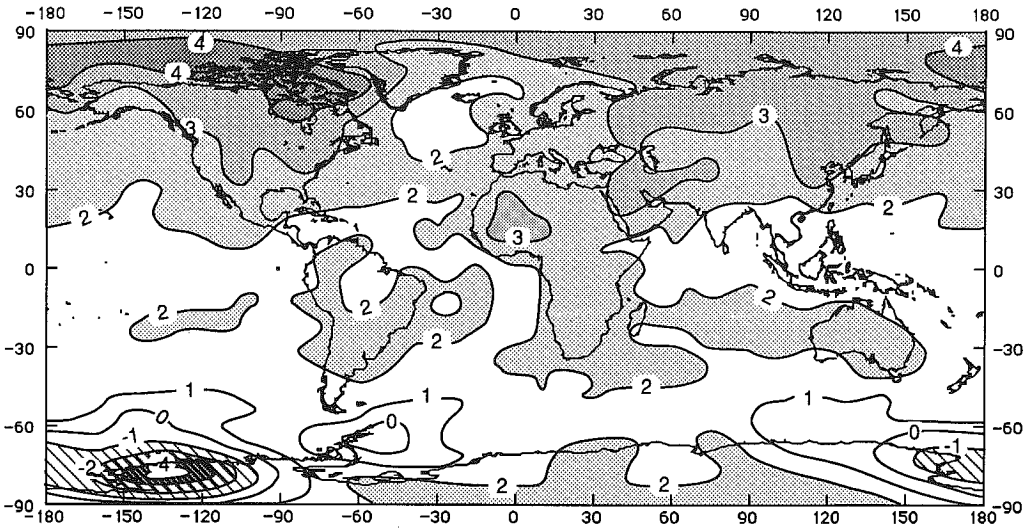

Fig 30.6. Map showing the predicted change in air temperature due to double CO_2 according to the model run of Stouffer, Manabe and Bryan (1989). Reprinted by permission of *Nature*. © 1989 MacMillan Magazines Ltd.

struction of Tushingham and Peltier (1991), based on regional sea-level curves and terrestrial reconstructions. The dating of the meltwater plumes in the Fram Strait (PS21295-4) and the Norwegian Sea (V27-60) suggests that the Barents ice sheet may have been responsible for the small initial rise of sea level between 16,000 and 15,000 ^{14}C years BP (Fig 30.1A) (Lehman *et al* 1991). It is clear from the meltwater plume records that the Laurentide ice sheet (Gerg13-31) was primarily responsible for the large sea-level increase between 12,300 and 11,800 ^{14}C years.

However, processes in the polar and subpolar regions may create apparent MWPs which are also tied to large-scale climate change (Broecker 1990a). For example, in the model simulation of Manabe and Stouffer (1988), in which they "turned-off" the thermohaline circulation, we have computed the estimated $\Delta\delta^{18}O$ based on their temperature and salinity anomaly maps (Fig 30.7). We can see from Figure 30.7C that oscillations of the thermohaline circulation can create apparent MWPs in the polar and subpolar regions up to −0.75‰. This is the magnitude of $\delta^{18}O$ anomalies in the Norwegian/Greenland Sea, which were assumed to be MWPs based solely on the low $\delta^{18}O$ anomalies (Jones & Keigwin 1988; Lehman *et al* 1991). The implications of these simulations are that low $\delta^{18}O$ anomalies could be either a product of meltwater plumes or temporary shutdown of the thermohaline circulation or both. Interestingly, all high-resolution deep-water records from the North Atlantic, as well as the Southern Ocean record of RC11-83, show an abrupt "switch-on" of the thermohaline cir-

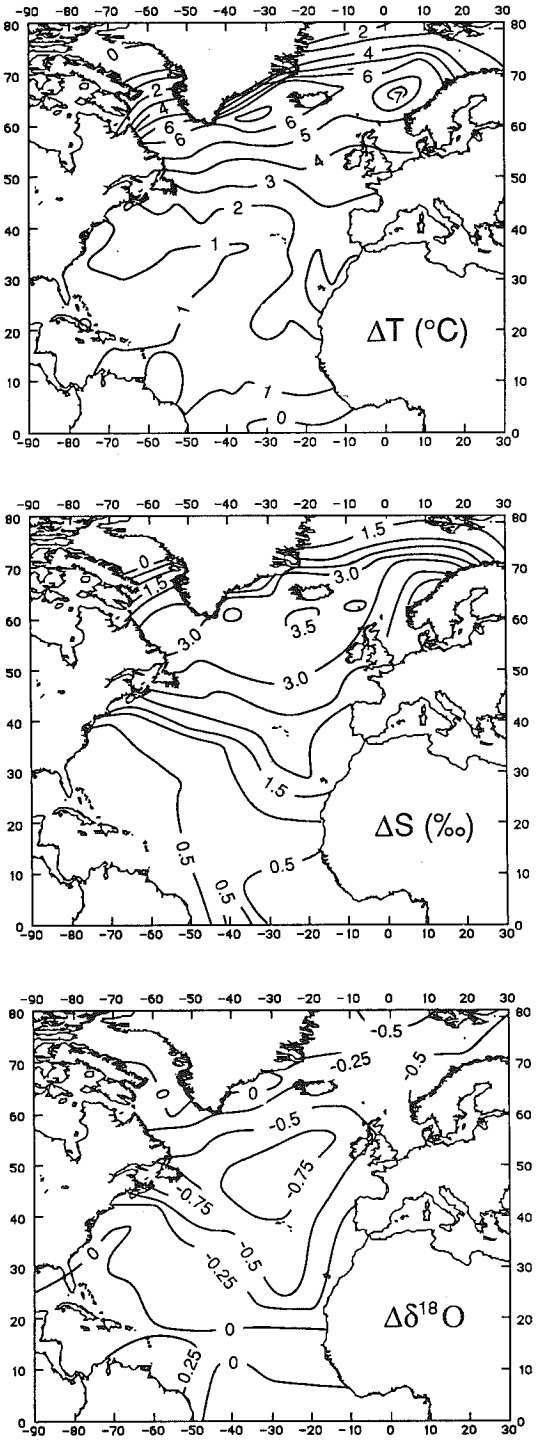

Fig 30.7. Maps showing the difference in North Atlantic surface-water temperature (A) and surface-water salinity (B) between model simulation with and without thermohaline circulation (from Manabe & Stauffer 1988). In the polar and subpolar latitudes, the $\delta^{18}O$ of sea water changes at a rate of −0.5‰ per unit salinity decrease compared to +0.22‰ for each degree temperature drop. The estimated difference in $\delta^{18}O$ shows that the effects of decreasing temperature and salinity tend to cancel out; however, in polar regions, the effects of decreasing salinity dominate (C).

culation at 13,000 ^{14}C years (Figs 30.4, 30.5). All three surface water records from the Norwegian Sea recorded a dramatic increase in δ^{18}O at approximately 13,000 ^{14}C years, which is consistent with the Manabe and Stouffer (1988) simulation (Fig 30.7). At 16,000 ^{14}C years, all of the Norwegian Sea surface-water records have high δ^{18}O values, which implies the thermohaline circulation is "switched-on" or possibly that sea ice conditions dominate the region. Our Southern Ocean core (RC11-83) indicates no net change in NADW flux until 13,000 ^{14}C years, which makes it difficult to explain the initial δ^{18}O decrease around 15,000 ^{14}C years. In summary, unless the δ^{18}O anomalies can be traced back to a point source with a large amplitude δ^{18}O signal, the possibility remains that they are artifacts of salinity changes due to oscillations of the thermohaline circulation.

This complex interplay between meltwater, marine precipitation and NADW has been developed into a conceptual model, known as the salt oscillator, by Broecker *et al* (1990a). The development of the salt oscillator model centered around the need for an explanation for rapid vegetation changes in western Europe and oscillations in the δ^{18}O record from Greenland ice cores and European lake cores during the Younger Dryas event. Broecker (1990) estimates that the annual production of NADW yields 4×10^{21} calories, which is approximately 10% of the atmospheric heat flux north of 50°N latitude (Carissimo, Oort & Vonder Haar 1985). The "switch-on" of NADW at 12,600 ^{14}C years (Charles & Fairbanks, ms) should have had immediate effects on European air temperatures according to GCM simulations. How this is transmitted to the catastrophic destruction of the Laurentide ice sheet between 12,300 and 11,800 ^{14}C years remains unresolved. A brief reduction in thermohaline circulation dated at 11,500 ^{14}C years (Fig 30.4) is a probable consequence of the MWP, centered at 12,000 ^{14}C years. This may be the best example of Broecker's "salt oscillator."

The influence of colder North Atlantic sea surface temperatures on atmospheric temperatures was simulated by Rind *et al* (1986) (Fig 30.8). Rind *et al* (1986) assigned winter sea surface temperatures that were approximately twice as cold as those simulated by Manabe and Stouffer's (1988) thermohaline circulation "off" mode. These extremely cold winter sea-surface temperatures resulted in winter air temperatures approximately 4°C cooler across Europe. It is important to note that the North American continent warmed slightly in this simulation, presumably due to a greater fraction of polar heat transport via the atmosphere to compensate for the loss in the oceanic heat transport. According to Stone (1978), the total meridional heat flux is primarily governed by physical factors other than the mode of transport (eg, ocean or atmosphere). Thus, a reduction in one mode will be at least partially compensated by the other.

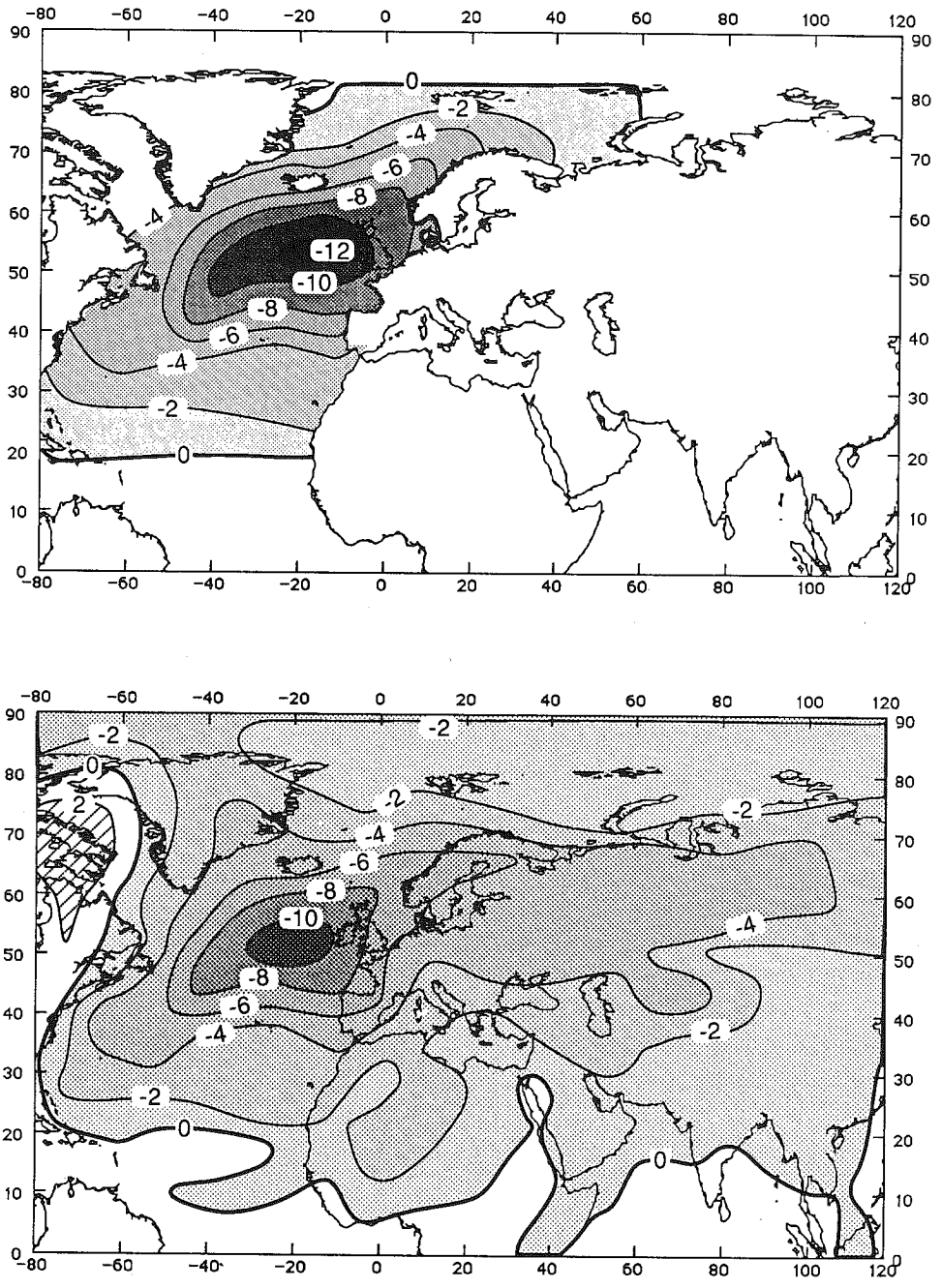

Fig 30.8. Maps showing influence of decreased winter sea-surface temperature in the North Atlantic on the winter air temperatures, as simulated by the Goddard Institute for Space Studies (GISS) atmospheric GCM (Rind *et al* 1986). Note that estimated air temperatures over Europe decrease while air temperatures over North America increase.

The simulation of Rind *et al* (1986) shows only a minor influence of NADW shut-down on the air temperatures over North America. More important, winter air temperatures are not generally considered critical for the massive ablation of ice sheets such as occurred in North America between 12,300 and 11,800 ^{14}C years. During the critical summer months, the northern North Atlantic Ocean is not an important source of heat to the North American continent. However, warm air masses are generally considered to be essential for the rapid ablation of an ice sheet (Oerlemans & van der Veen 1984). The strong winds associated with cyclones efficiently penetrate the temperature inversion layer over ice sheets, allowing warm air to erode the ice sheet. In summary, the thermohaline circulation status has direct effects on the winter air temperatures and vegetation history of Europe. However, the link to the Laurentide ice sheet must be indirect.

Thus, we must look to other indirect consequences of the "switch-on" of thermohaline circulation at 12,600 ^{14}C years on the ablation rates of the Laurentide ice sheet. It is important to note that the coincidence of the MWP computed from the Barbados sea-level curve and the measured meltwater plume from the Laurentide ice sheet demonstrates that the rise in sea level is due to a sudden change in the ablation rates, and not moisture supply rates to the Laurentide ice sheet.

One possible scenario that explains the coincidence of the "switch-on" of NADW and the catastrophic ablation of the Laurentide ice sheet is the simultaneous opening of the atmospheric corridor between the Laurentide ice sheet and Greenland (Fig 30.9). Today, the seasonally open water in the Labrador Sea and Baffin Bay, combined with the high elevation of Greenland to the east, causes cyclones to track northward to the Arctic, providing an important source of heat and moisture. During summer, the southeast coast of Greenland and Baffin Bay show the highest frequencies of cyclonic activity in the arctic (Reed & Kunkel 1960). The strong meridional flow of air greatly reduces the latitudinal climate differences along the west coast of Greenland (Putnins 1970; Vowinckel & Orvig 1970).

Today, the $\delta^{18}O$ difference between Dye 3 ice core in south Greenland and Camp Century in northwest Greenland is only 1.6‰, partially the result of the strong meridional flow of air. Fisher and Alt (1985) point out that the latitudinal gradient in $\delta^{18}O$ on the Greenland ice cap is an excellent measure of the meridional temperature gradients. Fairbanks (1990) applied this concept by comparing the difference in $\delta^{18}O$ between Dye 3 in south Greenland with Camp Century in northwest Greenland (Fig 30.10). During the Last Glacial Maximum, the difference between Dye 3 and Camp Century was 6‰, reflecting the zonal

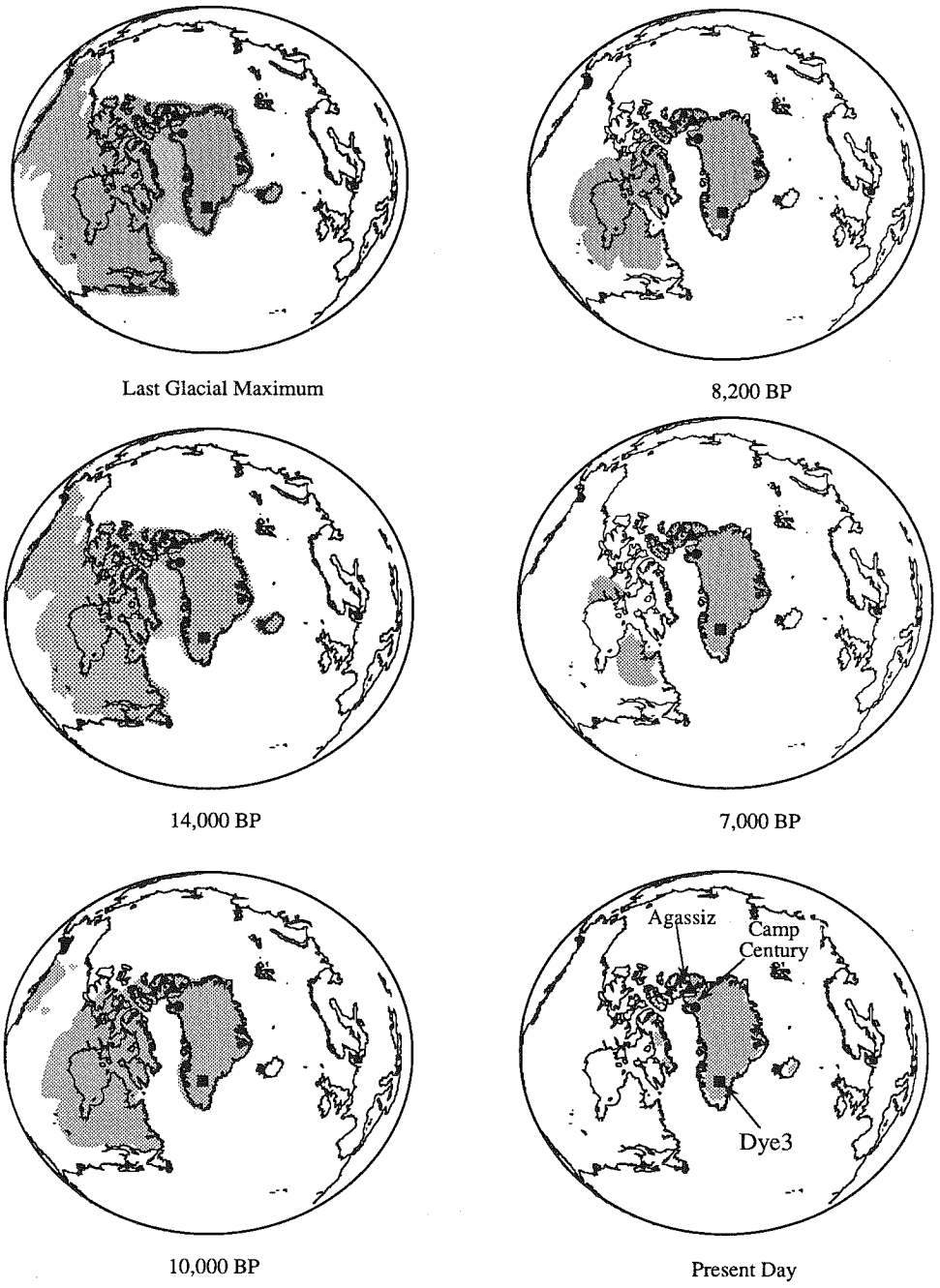

Fig 30.9. Maps of the deglaciation history of North America (modified after Denton & Hughes 1981).

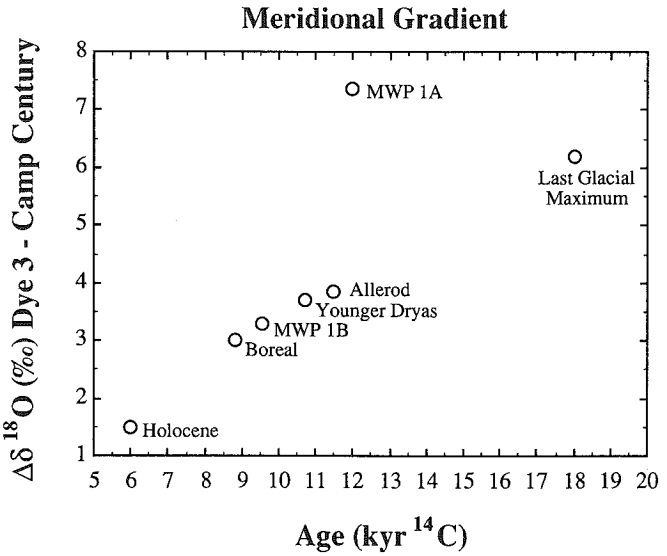

Fig 30.10. Meridional climate gradient along the west coast of Greenland estimated by the $\delta^{18}O$ difference between Dye 3 (southeast) and Camp Century (northwest) (from Fairbanks 1990). Assignment of ^{14}C chronozones is based upon the age model presented in Fairbanks (1990).

conditions documented by the CLIMAP group (1981). The $\Delta\delta^{18}O$ remained approximately 6‰ until it shifted suddenly to 4‰ during the Bølling/Allerød transition (Fairbanks 1990).

Although very little carbonate material is found in marine sediments of the Labrador Sea and Baffin Bay, Andrews *et al* (1990) successfully measured the stable isotope records from seven cores in this region, which are constrained by 35 ^{14}C dates. They found that the bulk of the sediment in their cores was deposited between 7000 and 11,500 ^{14}C years, and that there is a "conspicuous gap in ^{14}C dates between 13,300 ^{14}C years and 'old' basal dates" from their cores.

Therefore, evidence from the dated marine records support the ice core results, which indicate that the atmospheric corridor west of Greenland opened up approximately at 12,000 to 13,000 ^{14}C years. By 9500 ^{14}C years, ice-core results from Agassiz Ice Cap clearly indicate that the meridional heat flux through this corridor reached its maximum (Koerner & Fisher 1990), causing yearly melting of the ice cap (Fig 30.11). The melt-layer record on Agassiz ice cap also confirms that dramatic variations in the meridional heat flux along this corridor have occurred in the past.

Thus, the results from deep-sea and ice cores indicate that the massive disintegration of the Laurentide ice sheet at 12,000 ^{14}C years was coincident with a switch from zonal to meridional heat flux associated with the "switch-on" of the Atlantic thermohaline circulation (Broecker & Denton 1989) and the atmospheric

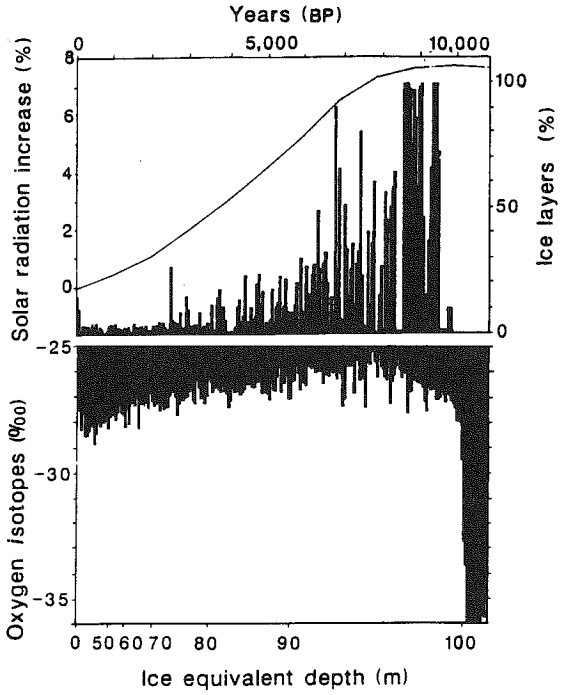

Fig 30.11. Percentage of annual melt layers that show melting averaged over 50-year intervals in ice core A-84 from the Agassiz Ice Cap at 1730 m elevation on Ellesmere Island, compared to local summer insolation record (from Koerner & Fisher 1990). Note intense melting peaked at approximately 9500 BP, according to the age model of Koerner and Fisher (1990). Work on Canadian ice caps showed that melt layers can be traced regionally between ice caps, and that melting correlates to late-summer sea-ice conditions in the region (Koerner 1989). Reprinted by permission of the author and *Science*. © 1989 AAAS.

heat pump *via* the Labrador Sea and Baffin Bay corridor. The proximity of the atmospheric corridor at the eastern edge of the Laurentide ice sheet, and the effectiveness of the atmospheric heat pump during critical summer months, makes this a likely trigger responsible for the catastrophic disintegration of the Laurentide ice sheet at 12,300 to 11,800 ^{14}C years.

CONCLUSIONS

Several new findings have impelled us to re-evaluate what is known about the amplifiers of glacial-to-postglacial climate change. These new results include:

1. The Barbados high-resolution sea-level record and global meltwater discharge curve (Fairbanks 1989, 1990);
2. The Barbados radiocarbon calibration for the deglaciation based on $^{230}Th/^{234}U$ dating by mass spectrometry (Bard *et al* 1990a);

3. New CO_2 data for Vostok, Dye 3 and Byrd ice cores (Barnola *et al* 1991; Staffelbach *et al* 1991);
4. AMS ^{14}C dating of NADW flux to the Southern Ocean (Charles & Fairbanks, ms), documenting the strength of the thermohaline circulation;
5. AMS-^{14}C-dated meltwater plumes in the circum-Atlantic ocean, which imply the sequential melting of the major ice sheets (Jones & Keigwin 1988; Broecker *et al* 1990; Lehman *et al* 1991);
6. New ^{14}C-dated marine cores in Baffin Bay, which indicate that seasonally open water was initiated approximately at 13,000 ^{14}C years (Andrews *et al* 1990).

Many amplifiers of postglacial climate change have been proposed. The timing and estimated magnitude of these amplifiers and their regional impact on climate are quite different. Compilation of AMS-^{14}C-dated meltwater plumes indicates that early deglaciation progressed from north to south. Using the Barbados radiocarbon calibration based on $^{230}Th/^{234}U$, we are able to place insolation, CO_2, ice-core climate records, deep-water reorganization and the Barbados meltwater curve on one time scale. The first major phase of deglaciation is coincident with the "switch-on" of the thermohaline circulation, as documented by AMS-^{14}C-dated carbon isotope records of deep-water circulation patterns. A probable consequence of the "switch-on" of the thermohaline circulation is seasonally open water in the Labrador Sea and Baffin Bay which in turn "switched-on" the "atmospheric heat pump" that operates along this corridor today. The implication for this study is that small changes in the oceanic heat flux in the Norwegian/Greenland Sea area may result in significant changes in the atmospheric heat transport through the much narrower corridor west of Greenland and immediately adjacent to the Laurentide ice sheet.

Although many aspects of the earth's energy budget can be researched using proxy records, we have virtually no tracers for many others. For example, insolation, water-mass and air-mass shifts, and atmospheric CO_2 and CH_4 are reasonably well known. However, we have no tracer for the most important greenhouse gas of all, water vapor. This chapter provides evidence for the causes of the first MWP dated at 12,000 ^{14}C years, but leaves explanations on the possible causes for the second MWP, dated at 9500 ^{14}C years, for another paper (Guilderson & Fairbanks, ms in preparation).

ACKNOWLEDGMENTS

We would like to thank Julie Cole, Tom Guilderson, Mimi Katz and Wallace Broecker for helpful suggestions and comments on this manuscript. This research was supported by NSF grants OCE88-19438 and ATM90-01139 to RGF.

REFERENCES

Andrews, JT, Evans, LW, Williams, KM, Briggs, WM, Jull, AJT, Erlenkeuser, H and Hardy, I 1990 Cryosphere/ocean interactions at the margins of the Laurentide Ice Sheet during the Younger Dryas chron: SE Baffin Shelf, Northwest Territories, 5. *Paleoceanography*.

Bard, E, Arnold, M, Duprat, J, Moyes, J and Duplessy, J-C 1987 Retreat velocity of the North Atlantic polar front during the last deglaciation determined by accelerator mass spectrometry. *Nature* 328: 791–794.

Bard, E, Hamelin, B, Fairbanks, RG and Zindler, A 1990a Calibration of the ^{14}C timescale over the past 30,000 years using mass spectrometric U-Th ages from Barbados corals. *Nature* 345: 405–410.

Bard, E, Hamelin, B, Fairbanks, RG, Zindler, A, Mathieu, G and Arnold, M 1990b U/Th and ^{14}C ages of corals from Barbados and their use for calibrating the ^{14}C time scale beyond 9000 years BP. *In* Yiou, F and Raisbeck, GM, eds, Proceedings of the 5th International Symposium on Accelerator Mass Spectrometry. *Nuclear Instruments and Methods* B52: 461–468.

Barnola, J-M, Pimienta, P, Raynaud, D and Korotkevich, YS 1991 CO_2-climate relationship as deduced from the Vostok ice core: a re-evaluation based on new measurements and on a re-evaluation of the air dating. *Tellus* 43B: 83–90.

Belanger, PE, Curry, WB and Matthews, RK 1981 Core-top evaluation of benthic foraminiferal isotopic ratios for paleooceanographic interpretations. *Palaeogeography, Palaeoclimatology, Palaeoecology* 33: 205-220.

Berger, A 1978 Long-term variation of caloric insolation resulting from the Earth's orbital elements. *Quaternary Research* 9: 139–167.

Boyle, E 1990 Effect of depleted planktonic $^{13}C/^{12}C$ on bottom water during periods of enhanced relative Antarctic productivity. *EOS* 71: 1357–1358.

_____1991 Quaternary ocean paleochemistry. In *US National Report to International Union of Geodesy and Geophysics 1987–1990*: 634–638.

Boyle, E and Keigwin, L 1987 North Atlantic thermohaline circulation during the past 20,000 years linked to high-latitude surface temperature. *Nature* 330: 35–40.

Broecker, WS 1984 Terminations. *In* Berger, AL, Imbrie, J, Hays, J, Kukla, G and Saltzman, B, eds, *Milankovitch and Climate*. Dordrecht, The Netherlands, Reidel: 687–698.

_____1990 Salinity history of the northern Atlantic during the last deglaciation. *Paleoceanography* 5: 459–467.

Broecker, WS, Bond, G, Klas, M, Bonani, G and Wölfli, W 1990a A salt oscillator in the glacial Atlantic?, 1, The concept. *Paleoceanography* 5: 469–478.

Broecker, WS and Denton, GG 1989 The role of the ocean-atmosphere reorganizations in glacial cycles. *Geochimica et Cosmochimica Acta* 53: 2465–2501.

Broecker, WS, Klas, M, Clark, E, Trumbore, S, Bonani, G, Wölfli, W and Ivy, S 1990b Accelerator mass spectrometric radiocarbon measurements on foraminifera shells from deep-sea cores. *Radiocarbon* 32(2): 119–133.

Broecker, WS, Peteet, D and Rind, D 1985 Does the ocean-atmosphere have more than one stable mode of operation? *Nature* 315: 21–25.

Bryan, F 1986 High-latitude salinity effects and interhemispheric thermohaline circulations. *Nature* 323: 301–304.

Carissimo, BC, Oort, AH and Vonder Haar, TH 1985 Estimating the meridional energy transports in the atmosphere and ocean. *Journal of Physical Oceanography* 15: 82–91.

Chappell, J and Polach, H 1991 Post-glacial sea-level rise from a coral record at Huon Peninsula, Papua New Guinea. *Nature* 349: 147–149.

Charles, CD and Fairbanks, RG 1990 Glacial-interglacial changes in the isotopic

gradients of Southern Ocean surface water. *In* Bleil, U and Thiede, J, eds, The Geologic History of Polar Oceans: Arctic *vs* Antarctic. *NATO ASI Series* 308. Dordrecht, The Netherlands, Kluwer Academic Publishers: 519–538.

_____(ms) North Atlantic deep water and its climate effects over the last deglaciation: Evidence from Southern Ocean isotope records. Submitted to *Nature*.

CLIMAP Project Members 1981 *Geological Society of America Map and Chart Series* MC 36.

Dansgaard, W, White, JW and Johnson, SL 1989 The abrupt termination of the Younger Dryas climate event. *Nature* 339: 532–534.

Denton, GH and Hughes, DJ 1981. *The Last Great Ice Sheets*. New York, Wiley-Interscience.

Edwards, RL, Taylor, FW and Wasserburg, GJ 1988 Dating earthquakes with high-precision thorium-230 ages of very young corals. *Earth and Planetary Science Letters* 90: 371–381.

Emiliani, C, Rooth, C and Stipp, JJ 1978 The late Wisconsin flood into the Gulf of Mexico. *Earth and Planetary Science Letters* 41: 159–162.

Epstein, S, Buchsbaum, R, Lowenstam, HA and Urey, HC 1953 Revised carbonate-water isotopic temperature scale. *Geologic Society of America Bulletin* 64: 1315–1326.

Fairbanks, RG 1989 A 17,000-year glacio-eustatic sea level record: Influence of glacial melting rates on the Younger Dryas event and deep-ocean circulation. *Nature* 3421: 637–642.

_____1990 The age and origin of the "Younger Dryas climate event" in Greenland ice cores. *Paleoceanography* 5: 937–948.

Fisher, D and Alt, BT 1985 A global oxygen isotope model – semi-empirical zonally averaged. *Annals of Glaciology* 7: 117–124.

Gordon, A 1986 Interocean exchange of thermocline water. *Journal of Geophysical Research* 91: 5037–5046.

Hays, JD, Imbrie, J and Shackleton, NJ 1976 Variations in the Earth's orbit, pacemaker of the Ice Ages. *Science* 194: 1121-1132.

Jansen, E and Veum, T 1990 Two-step deglaciation: timing and impact on North Atlantic Deep Water circulation. *Nature* 343: 612–616.

Jones, G and Keigwin, LD 1988 Evidence from Fram strait (78°N) for early deglaciation. *Nature* 336: 56–59.

Keigwin, LD 1987 North Pacific deep water formation during the latest glaciation, *Nature* 330: 362–364.

Keigwin, LD and Jones, GA 1989 Glacial-Holocene stratigraphy, chronology, and paleoceanographic observations on some North Atlantic sediment drifts. *Deep-Sea Research* 36: 845–867.

Kennett, JP and Shackleton, NJ 1975 Laurentide ice sheet meltwater recorded in Gulf of Mexico deep-sea cores. *Science* 188: 147–150.

Koerner, RM 1989 Ice core evidence for extensive melting of the Greenland ice sheet in the last interglacial. *Science* 244: 964–968.

Koerner, RM and Fisher, DA 1990 A record of Holocene summer climate from a Canadian high-Arctic ice core. *Nature* 343: 630–631.

Kroopnick, P 1985 The distribution of carbon-13 in the world oceans. *Deep Sea Research* 32: 57–84.

Labracherie, M, Labeyrie, LD, Duprat, J, Pichon, J, Bard, E, Arnold, M and Duplessy, JC 1989 The last deglaciation in the Southern Ocean. *Paleoceanography* 4: 629–638.

Lehman, SJ, Jones, GA, Keigwin, LD, Andersen, ES, Butenko, G and Ostmo, S-R 1991 Initiation of Fennoscandian ice-sheet retreat during the last deglaciation. *Nature* 349: 513–516.

Leventer, A, Williams, DF and Kennett, JP 1982 Dynamics of the Laurentide ice sheet during the last deglaciation: evidence from the Gulf of Mexico. *Earth and Planetary Science Letters* 59: 11–17.

Levitus, S 1982 Climatological atlas of the world ocean. *NOAA Professional Paper* 13. Washington, DC, US Government Printing Office: 173 p.

Lorius, C, Jouzel, J, Raynaud, D, Hansen, J and Le Treut, H 1990 The ice-core record: Climate sensitivity and future greenhouse warming. *Nature* 347: 139–145.

Maier-Reimer, E and Mikolajewicz, U 1989 Experiments with an OGCM on the cause of the Younger Dryas. *In* Ayala-Castanares, A, Wooster, W and Yanez-Arancibia, A, eds, *Oceanography 1988.* Mexico, UNAM Press: 87–100.

Manabe, S and Stouffer, RJ 1988 Two stable equilibria of a coupled ocean-atmosphere model. *Journal of Climate* 1: 841–866.

Milankovitch, M 1941 *Canon of Insolation and the Ice Age Problem.* Belgrade, Royal Serbian Academy. (Translation, Israel Program for Scientific Translation, Jerusalem, 1969).

Mix, AC and Fairbanks, RG 1985 North Atlantic surface-ocean control of Pleistocene deep-ocean circulation. *Earth and Planetary Science Letters* 73: 231–243.

Neftel, A, Oeschger, H, Staffelbach, T and Stauffer, B 1988 The CO_2 record in the Byrd ice core 50,000–5,000 years BP. *Nature 33*: 609–611.

Oerlemans, J and van der Veen, CJ 1984 *Ice Sheets and Climate.* Boston, D Reidel Company: 217 p.

Oppo, DW and Fairbanks, RG 1987 Variability in the deep and intermediate water circulation of the Atlantic Ocean during the past 25,000 years: Northern Hemisphere modulation of the Southern Ocean. *Earth and Planetary Science Letters* 86: 1–15.

_____1990 Atlantic Ocean thermohaline circulation of the last 150,000 years: Relationship to climate and atmospheric CO_2. *Paleoceanography* 5: 277–288.

Paterson, WSB and Hammer, C 1987 Ice core and other glaciological data. *In* Ruddiman, WF and Wright, HE, eds, *The Geology of North America K3, North America and Adjacent Oceans During the Last Deglaciation.* The Geological Society of America: 91–109.

Peltier, WR 1990 Glacial isostatic adjustment and relative sea level change. In *Studies in Geophysics.* Washington, DC, National Academy Press: 37–51.

Prell, W 1984 Variation of monsoonal upwelling: response to changing solar radiation. *In* Hansen, JE and Takahashi, T, eds, *Climate Processes and Climate Sensitivity.* Geophysics Monographs 29, Maurice Ewing Volume 5: 48–57.

Putnins, P 1970 The climate of Greenland. *In* Orvig, S, ed, *Climates of Polar Regions, World Survey of Climatology.* New York, Elsevier: 3–128.

Reed, RJ and Kunkel, BA 1960 The arctic circulation in summer. *Journal of Meteorology* 17: 489–506.

Rind, D, Peteet, D, Broecker, WS, McIntyre, A and Ruddiman, WF 1986 The impact of cold North Atlantic sea surface temperatures on climate: Implications to the Younger Dryas cooling (11–10K). *Climate Dynamics* 1: 3–33.

Rooth, C 1982 Hydrology and ocean circulation. *Progress in Oceanography* 1(1): 131–149.

Staffelbach, T, Stauffer, B, Sigg, A and Oeschger, H 1991 CO_2 measurements from polar ice cores: more data from different sites. *Tellus* 43B: 91–96.

Stauffer, B, Neftel, A, Oeschger, H and Schwander, J 1985 CO_2 concentration in air extracted from Greenland ice samples. *In* Greenland Ice Core: Geophysics, Geochemistry and the Environment. *Geophysics Monographs* 33: 85–89.

Stommel, H 1961 Thermohaline convection with two stable regimes of flow. *Tellus* 13: 224–230.

Stone, PH 1978 Constraints on dynamical transports of energy on a spherical planet. *Dynamics of Oceans and Atmosphere* 2: 123–139.

Stouffer, RJ, Manabe, S and Bryan, K 1989 Interhemispheric asymmetry in climate response to a gradual increase of atmospheric CO_2. *Nature* 342: 660–662.

Stuiver, M, Kromer, B, Becker, B and Ferguson, CW 1986 Radiocarbon age calibration back to 13,300 years BP and the ^{14}C age matching of the German oak and US bristlecone pine chronologies. *In* Stuiver, M and Kra, RS, eds, Proceedings of the 12th International ^{14}C Conference. *Radiocarbon* 28(2B): 969–979.

Tushingham, AM and Peltier, WR 1991 ICE-G: A new global model of late Pleistocene deglaciation based upon geophysical predictions of post-glacial relative sea level change. *Journal of Geophysical Research* 96: 4497–4523.

Vowinckel, E and Orvig, S 1970 The climate of the North Polar Basin. *In* Orvig, S, ed, *Climates of Polar Regions, World Survey of Climatology*. New York, Elsevier: 3–128.